Manipulation of a two-photon state in a $\chi^{(2)}$-modulated nonlinear waveguide array

Y. Yang, P. Xu,* L. L. Lu, and S. N. Zhu

National Laboratory of Solid State Microstructures and School of Physics, Nanjing University, Nanjing 210093, China

(Received 5 April 2014; published 21 October 2014)

We propose to engineer the quantum state in a high-dimensional Hilbert space by taking advantage of a $\chi^{(2)}$-modulated nonlinear waveguide array. By varying the pump condition and the waveguide array length, the momentum correlation between the signal and idler photons can be manipulated, exhibiting bunching, antibunching, and the evolution between these two states, which are characterized by the Schmidt number. We find the Schmidt number is dependent on a structure parameter, namely the ratio of the array length and the number of channels pumped. By designing the linear profile waveguide array, the degree of spatial entanglement shows a periodic relationship with the slope of linear profile, during which a high degree of position-bunching state is suggested. The two-photon self-focusing effect is disclosed when the $\chi^{(2)}$ modulation in the waveguide array contains a parabolic profile, which can be designed for efficient coupling between a waveguide array and fibers. These results shed light on a feasible way to achieve desirable quantum state on a single waveguide chip by a compact engineering of $\chi^{(2)}$ and also suggest a degree of freedom for quantum walk and other related applications.

DOI: 10.1103/PhysRevA.90.043842 PACS number(s): 42.50.Dv, 42.65.Lm, 03.67.Mn, 03.65.Ud

I. INTRODUCTION

Photonic waveguide array (WA) supplies a unique platform for the study of the linear or nonlinear optical phenomena [1]. The periodicity of refraction index and nonlinearity enable one to mould the flow of light, exhibiting the diffraction behavior characteristic of that encountered in discrete systems [2]. Bloch oscillations [3–5], discrete solitons [6,7], Talbot effect [8], dynamic localization [9–12], Rabi oscillations [13,14], etc., have been observed in waveguide arrays. Recently, the WA is introduced into the field of quantum walk to demonstrate the continuous quantum walk of single-photon and entangled photon pairs [15–17]. These studies will promote the applications of quantum walk in the design and implementation of quantum algorithms. In 2011, another type of quantum walk was proposed [18]. By designing the quadratic $\chi^{(2)}$ WA, the entangled photon pairs can be generated and coupled during the spontaneous parametric down conversion (SPDC) process, which dispenses with the external single- or multiphoton source and results in peculiar properties of quantum walk. From a different perspective, the $\chi^{(2)}$ WA presents the prospects in engineering the quantum state in high-dimensional Hilbert space, by either changing the amplitude or phase profile of the pump. The $\chi^{(3)}$ WA was also suggested for engineering the entangled photons, leading to different characters of quantum walk [19]. Then spatiospectral properties of SPDC in WA were further considered [20].

In this paper, we propose to engineer the quantum state by taking advantage of a $\chi^{(2)}$-modulated nonlinear waveguide array, wherein the longitudinal $\chi^{(2)}$ modulation ensures the quasi-phase-matching (QPM) condition of the SPDC process for the entangled photons generation, while the transverse $\chi^{(2)}$ modulation supplies a unique way to manipulate the two-photon spatial correlation. By verifying the profile of the initial position of each $\chi^{(2)}$-modulated waveguide, the transverse $\chi^{(2)}$-modulation function will be transferred into a two-photon mode function, resulting in two-photon bunching, antibunching, the evolution between them, or a self-focusing effect. By calculating the Schmidt number, the entanglement degree of the engineered state is evaluated, showing a characteristic relationship with the WA length and the pump parameters. Following this way, the high degree of spatial entanglement is suggested. This work sheds light on a feasible way to achieve desirable quantum state on a single chip by a compact engineering of $\chi^{(2)}$. This also suggests another degree of freedom for quantum walk and other related applications.

This paper is organized as follows. In Sec. II, the general two-photon state in a $\chi^{(2)}$-modulated nonlinear waveguide array is given. In Sec. III, the manipulation of spatial correlation for the photon pair is achieved by changing the pump condition and the waveguide array length. The degree of spatial entanglement is characterized by the Schmidt number. In Sec. IV, the WA with linear profile $\chi^{(2)}$ modulation is studied, during which a high degree of a position-bunching state is suggested. In Sec. V, the parabolic profile of $\chi^{(2)}$ modulation is discussed, which leads to the two-photon self-focusing effect outside the waveguide array. Discussions about the loss are given in Sec. VI and conclusions are drawn in Sec. VII.

II. GENERAL TWO-PHOTON STATE FROM A $\chi^{(2)}$-MODULATED NONLINEAR WAVEGUIDE ARRAY

First of all, we will give a general form of the two-photon state from a $\chi^{(2)}$-modulated nonlinear waveguide array. The WA is designed as follows. The WA substrate material can be lithium niobate (LN) or lithium tantalate (LT), etc. These materials can be fabricated into waveguides by using either a proton-exchange or titanium-diffusion method. More importantly, such material can be domain engineered, i.e., $\chi^{(2)}$ modulation is allowed to supply an additional "momentum" for satisfying the momentum conservation during the SPDC process for the entangled photons generation, namely a quasi-phase-matching (QPM) condition. The period of $\chi^{(2)}$ modulation can be designed to match the requirement for different wavelength photons within the wide transparent

*Corresponding author: pingxu520@nju.edu.cn

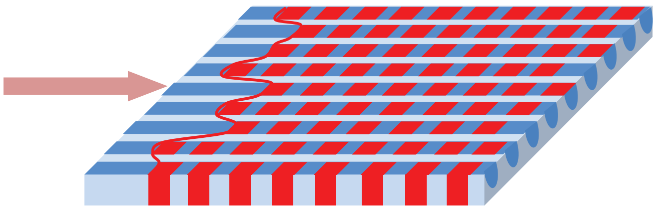

FIG. 1. (Color online) Sketch of the $\chi^{(2)}$-modulated nonlinear waveguide array is given. The deep blue areas are proton-exchanged waveguide channels and the red shows the domain reversal area. The red curved line is the initial position profile of the domain.

window of LN or LT materials. Here in this work we assume the WA is periodically poled along the propagation direction, while the initial position of each waveguide is engineered according to certain functions. The $\chi^{(2)}$ modulation in such WA is generally described as

$$\chi^{(2)}(z,x_0) = U(x_0)d_{\text{eff}} \sum_m F(G_m)e^{iG_m[z+f(x_0)]}, \quad (1)$$

where n represents the no. n waveguide channel. $G_m = \frac{2m\pi}{\Lambda}$ is the m-order reciprocal vector resulting from the periodic modulation of $\chi^{(2)}$ with a period of Λ along the z direction. Here only G_1 is competent for the QPM SPDC process. d_{eff} is the effective second-order nonlinear susceptibility. $U(x_0)$ denotes the amplitude profile for transverse $\chi^{(2)}$ modulation. Here we assume $U(x_0)$ is constant. $F(G_m)$ is the Fourier coefficient. $f(x_0)$ is the initial position profile of the domain (the red curved line shown in Fig. 1). We will discuss the two-photon state under different $f(x_0)$ in the following sections. The interaction Hamiltonian in the above WA can be described as

$$H_I = \sum_n \int dz\, \chi^{(2)}(z,x_0)E^{(+)}_{p,n}E^{(-)}_{s,n}E^{(-)}_{i,n} + \text{H.c.} \quad (2)$$

$E^{(+)}_{p,n}, E^{(-)}_{s,n}, E^{(-)}_{i,n}$ are the pump, signal, and idle field, respectively, in the no. n waveguide, where the pump is considered as a classical field while the signal and idler are treated quantum mechanically,

$$E^{(+)}_{p,n} = \int d\kappa_p A_p(\kappa_p)e^{in\kappa_p}e^{i\beta_p z - i\omega_p t}, \quad (3)$$

$$E^{(-)}_{s(i),n} = \int d\kappa_{s(i)}e^{in\kappa_{s(i)}}e^{-i\beta_{s(i)}z+i\omega_{s(i)}t}\hat{a}^\dagger_{s(i)}(\kappa_{s(i)}), \quad (4)$$

where $\kappa_{p,s,i} = k_{p,s,i}d$ is the reduced transverse wave vector which is the product of transverse wave vector $k_{p,s,i}$ and the transverse separation d of WA. $A_p(\kappa_p) = [\text{sinc}(\frac{w}{d}\kappa_p)\text{comb}(\kappa_p)] * \text{sinc}[N\kappa_p]$ is the pump mode function which is the Fourier transform of the pump condition, namely $A_p(x_0) = [\text{rect}(\frac{x_0}{w}) * \text{comb}(\frac{x_0}{d})]\text{rect}[\frac{x_0}{Nd}]$. N is the total number of pumped waveguide channels and w is the width of every waveguide channel. $\beta_{p,s,i}$ is the longitudinal wave vector as a function of reduced transverse wave vector $\kappa_{p,s,i}$ and frequency $\omega_{p,s,i}$,

$$\beta_{s,i} = \beta^{(0)}(\omega_{s,i}) + 2C_{s,i}\cos(\kappa_{s,i}). \quad (5)$$

$C_{s,i}$ is a coupling parameter of the waveguide for the signal or idler photon. $\beta^{(0)}(\omega_{s,i}) = n_{\text{eff}}(\omega_{s,i})\omega_{s,i}/c$ is the propagation constant defined by the effective refraction index $n_{\text{eff}}(\omega_{s,i})$ in the waveguide. For the pump, the evanescent wave coupling between adjacent waveguides is neglected. By the second quantization method and Bloch waves basis expansion in the WA, the two-photon state is obtained,

$$|\Psi\rangle \sim \int\int d\kappa_s d\kappa_i A_p(\kappa_s,\kappa_i)e^{iG_1 f(x_0)}\text{sinc}\left(\frac{\Delta\beta L}{2}\right) \times e^{-i\frac{\Delta\beta L}{2}}\hat{a}^\dagger_s\hat{a}^\dagger_i|0,0\rangle. \quad (6)$$

L is the length of the array. $\Delta\beta = \Delta\beta^0(\omega_s,\omega_i) - 2C_s\cos(\kappa_s) - 2C_i\cos(\kappa_i)$ is the phase mismatch. Here we consider the type-0 degenerate SPDC process, which means the signal and idle photon share the same frequency and polarization, so $C_s = C_i = C$. The zero-order phase mismatch $\Delta\beta^0(\omega_s,\omega_i) = \beta^0(\omega_p) - \beta^0(\omega_p) - \beta^0(\omega_p) - G_1$ is designed to be zero. Then the phase mismatch is reduced into $\Delta\beta = 4C\ \cos(\frac{\kappa_s+\kappa_i}{2})\cos(\frac{\kappa_s-\kappa_i}{2})$.

III. SPATIAL CORRELATION OF TWO-PHOTON STATE IN THE HOMOGENEOUS WAVEGUIDE ARRAY

Here, we consider a homogeneous WA, i.e., $f(x_0) = 1$. The two-photon amplitude $\varphi(\kappa_s,\kappa_i) = A_p(\kappa_s,\kappa_i)\text{sinc}(\frac{\Delta\beta L}{2})e^{-i\frac{\Delta\beta L}{2}}$, describing the spatial correlation between entangled two photons in the WA, shows a joint connection between the pump mode function and phase-mismatching term. When only considering the first Brillouin zone of the signal and idler, the pump condition gives a momentum antibunching correlation following $\kappa_s + \kappa_i = 0$ when the $N \to \infty$, while the phase-mismatching term presents either bunching or antibunching correlation by requiring $\kappa_s + \kappa_i = \pm\pi$ or $\kappa_s - \kappa_i = \pm\pi$ when $L \to \infty$. For a practical case, the dominant bunching or antibunching effect is decided by a comparison between the bandwidth of the pump term and that of the phase-mismatching term, which are determined by the number of waveguides N and the length L of WA. For a fixed N or L, verifying L or N will bring a continuous evolution from two-photon bunching to an antibunching state.

Figure 2 shows the momentum correlation with different WA lengths $L = 0.3L_z, 0.9L_z, 4L_z$ (L_z is the coupling length for two adjacent waveguides). The pump is assumed to cover $n = 0, \pm 1, \pm 2, 3$ waveguides. The first column of Fig. 2 shows the signal-idler momentum anticorrelation decided by the pump condition. The second column presents a phase-mismatching term [sinc term in Eq. (6)]. The bandwidth of $\kappa_s + \kappa_i$ or $\kappa_s - \kappa_i$ is obviously getting smaller when the WA's length increases as shown in the middle column of Fig. 2. The product of the pump mode function and phase-mismatching term shows an evolution from antibunching to bunching in momentum space, which is depicted in the right column of Fig. 2. This phenomenon tells us that the spatial correlation varies for different propagation lengths of WA.

To be more vivid, the Schmidt number $K = \frac{1}{\sum_m \lambda_m^2}$ (where λ_m is the eigenvalue of reduced density matrices for a photon pair expanded by Schmidt modes) [21,22] as a function of the ratio L/L_z with different pump conditions is described as shown in Fig. 3. In this numerical simulation, a method for calculating the Schmidt number [23] is applied. As

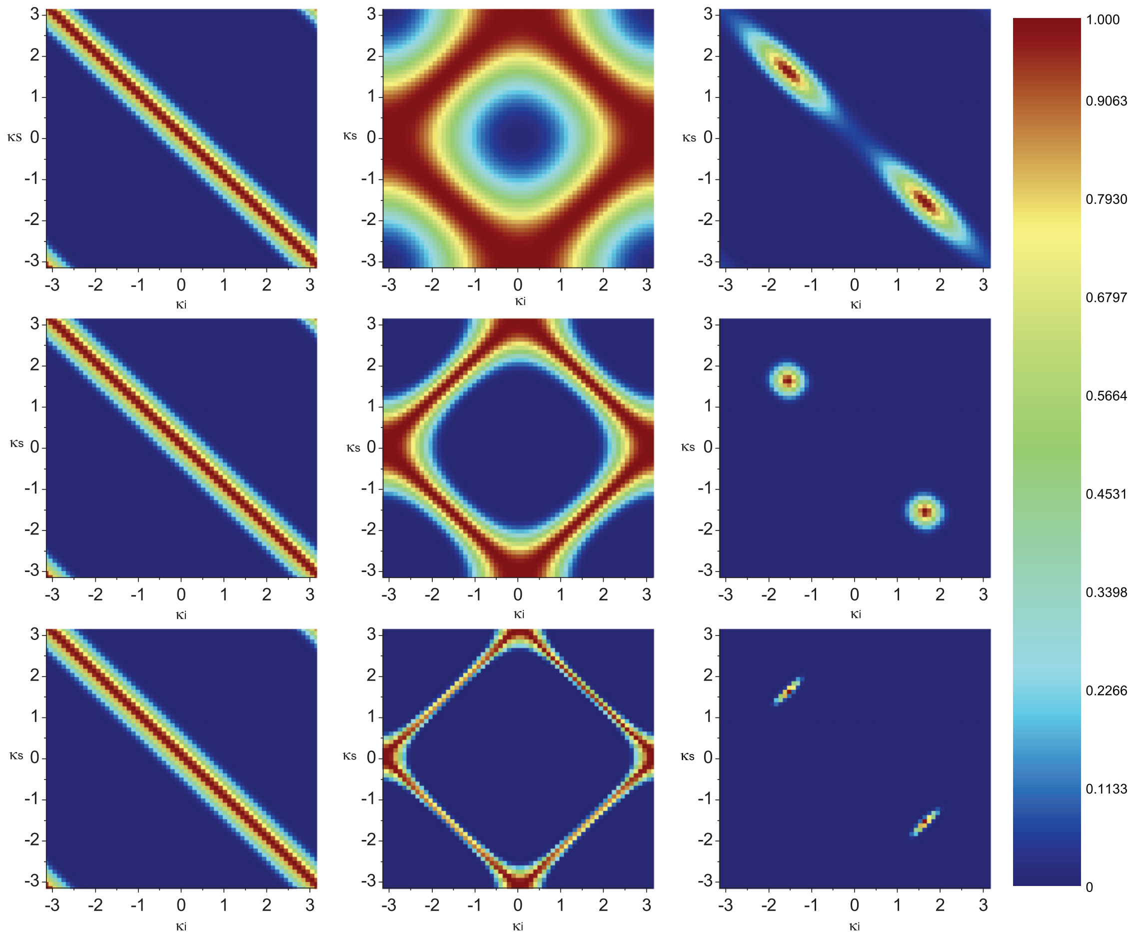

FIG. 2. (Color online) Pump condition, phase mismatch, and the momentum correlation is demonstrated when the pump condition is $n = 0, \pm 1, \pm 2, 3$ under three array lengths $L = 0.3L_z, 0.9L_z, 4L_z$.

shown by Ref. [23], the Schmidt number can be described as $K = \frac{X^2}{Y}$, where $X = \int d\kappa_s \int d\kappa_i |\varphi(\kappa_s,\kappa_i)|^2$ and $Y = \int d\kappa_s \int d\kappa_i \int d\kappa_s' \int d\kappa_i' [\varphi(\kappa_s,\kappa_i)\varphi(\kappa_s',\kappa_i')\varphi^*(\kappa_s,\kappa_i')\varphi^*(\kappa_s',\kappa_i)]$. According to Fig. 3, the entanglement degree of the photon pair decreases first and then increases as the length of the array enlarging. And the minimal Schmidt number stands for the near-uncorrelated photon pair state, namely the entanglement degree is lowest. Besides, as the number of pumped waveguide channels increases (N turns larger), the near-uncorrelated point shifts to a larger length of the array. This phenomenon can be explained as follows: as suggested from Refs. [21] and [24], the near-uncorrelated condition corresponds to a comparative bandwidth between the pump mode function and the phase-mismatching term. Since they both follow the monotonous relationship with N or L, therefore, when N increases, the near-uncorrelated condition moves to a larger L/L_z. From Fig. 3, to engineer the bunching or antibunching state, for a fixed N, we prefer an extremely short or a long WA.

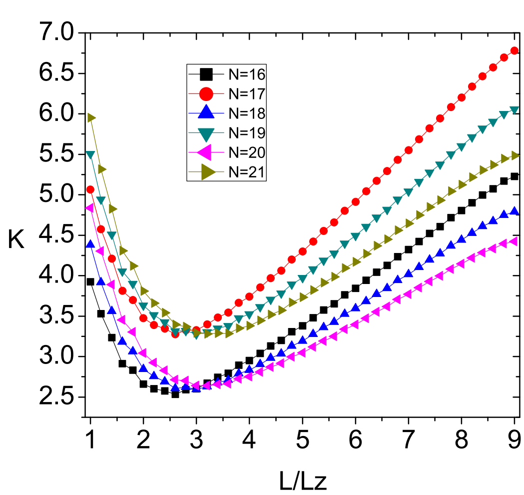

FIG. 3. (Color online) Schmidt number is given as a function of ratio L/L_z when the number of pumped waveguide channels N varies from 16 to 21.

In Figs. 4(a) and 4(b), by choosing the single structure parameter, namely the ratio of the array length and the number of channels $(L/L_z)/N$, we find the unique dependance of Schmidt number on this parameter, i.e., no matter the absolute value of L/L_z and N, the Schmidt number is only decided by the ratio of them. The Schmidt number always decreases first and then increases as the ratio enlarging. The smallest Schmidt number corresponding to a near-uncorrelated state for odd N is approached when the ratio reaches around 0.15. For even N, although the Schmidt number shows a similar

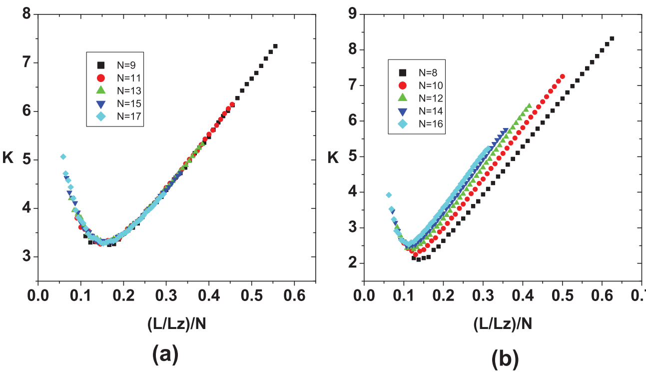

FIG. 4. (Color online) Schmidt number is given as a function of the ratio $(L/L_z)/N$ when the number of pumped waveguide channels N varies from 8 to 17. The Schmidt number for odd and even N is plotted separately.

dependance on the structure parameter as the case of odd N, they do not overlap. Meanwhile, for different N (even), the Schmidt number differs a little. These differences may result from the different pump mode functions. From Fig. 4(b), we also know when N (even) is getting larger, the Schmidt number tends to show a unique dependance on the ratio $(L/L_z)/N$, which is similar with the odd N case.

IV. TWO-PHOTON SPATIAL CORRELATION IN THE LINEAR PROFILE WAVEGUIDE ARRAY

In this section, we consider the initial position of $\chi^{(2)}$ modulation is a linear function of n,

$$f(x_0) = ax_0. \tag{7}$$

a describes the slope of such titled WA and $x_0 = nd$ is discrete. Then the two-photon state has the following form:

$$|\Psi\rangle \sim \int\int d\kappa_s d\kappa_i \sum_n e^{-in(\kappa_s+\kappa_i+G_1 ad)}\text{sinc}\left(\frac{\Delta\beta L}{2}\right) \times e^{-i\frac{\Delta\beta L}{2}}\hat{a}_s^\dagger \hat{a}_i^\dagger |0,0\rangle. \tag{8}$$

As discussed before, the phase-mismatching function inherently sets a constraint to the relationship between κ_s and κ_i which is antibunching or bunching. In this case, the pump mode function $\sum_n e^{-in(\kappa_s+\kappa_i+G_1 ad)}$ turns to $2\pi\sum_M \delta(\kappa_s+\kappa_i+G_1 ad-2\pi M)$. Specifically when $G_1 ad$ is designed to be π, we achieve $2\pi\sum_M \delta(\kappa_s+\kappa_i+\pi-2\pi M)$, namely $\kappa_s+\kappa_i=\pm\pi$ for $M=0,1$ in the first Brillouin zone, which overlaps with the antibunching relation determined by the phase-mismatching function as shown by the upper two pictures of Fig. 5. The momenta of the signal and idler photon are then anticorrelated. The position of the photon pair, calculated by $G^{(2)}(n_s,n_i) = |\int\int d\kappa_s d\kappa_i e^{i\kappa_s n_s} e^{i\kappa_i n_i} A_p(\kappa_s,\kappa_i)\text{sinc}(\frac{\Delta\beta L}{2})e^{-i\frac{\Delta\beta L}{2}}|^2$ should be correlated. The corresponding momentum and position correlations of the photon pair are demonstrated by the lower two in Fig. 5, which exhibit a well-defined momentum antibunching and position bunching effect. When compared with the homogeneous WA, the sum of signal and idler momentum is shifted by $G_1 ad$, which brings different characters to the spatial correlation. By evaluating the

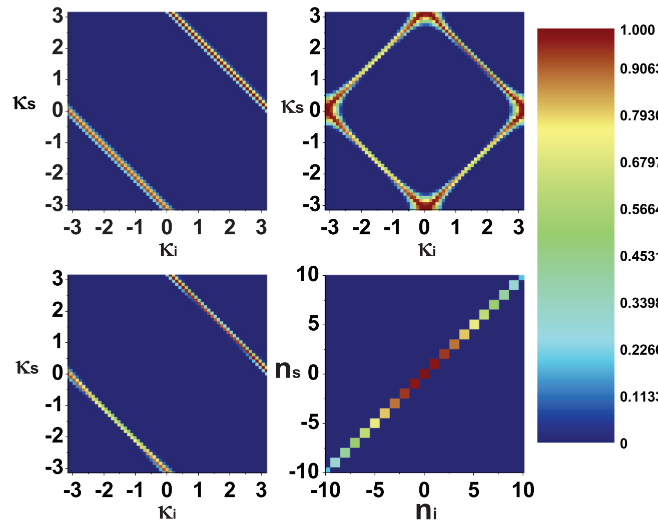

FIG. 5. (Color online) Momentum and position correlation of a two-photon state generated from the WA with linear domain profile.

Schmidt number as a function of $G_1 ad$ in Fig. 6, we find the Schmidt number represents itself periodically. The period is 2π, which is consistent with the periodicity of pump mode function in Eq. (8). The Schmidt number approaches as high as 21.82. This suggests a feasible way to engineer a high degree of spatial entanglement. As proposed in Ref. [18], the high degree of position antibunching state can be achieved by pumping no. 0 and no. 1 waveguide channels (here we calculate the Schmidt number to be 8.01). But the high-degree position bunching state can hardly be approached by just choosing different pumping channels or setting the phase difference between them. The slope of linear profile a supplies as an alternative a parameter to engineer the two-photon state from the WA, especially for the high degree of the position bunching state.

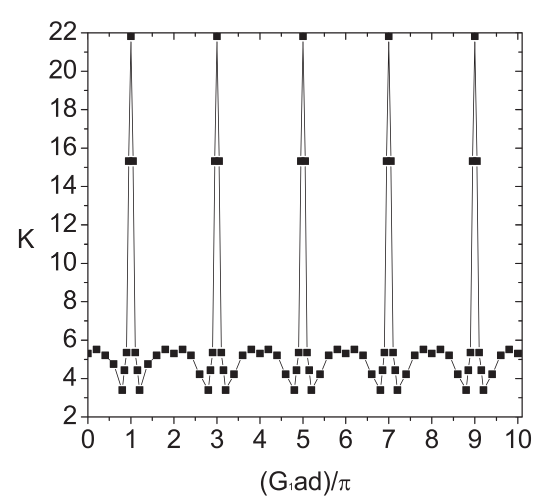

FIG. 6. Schmidt number when the slope of the linear profile increases with all waveguide channels pumped and the length of the array is $L = 10Lz$.

V. TWO-PHOTON SPATIAL CORRELATION IN A PARABOLIC PROFILE WAVEGUIDE ARRAY

Now we discuss another type of transverse domain modulation. When the transverse profile is parabolic following $f(x_0) = bx_0^2$, the two-photon state turns to

$$|\Psi\rangle \sim \int\int A_p(\kappa_s,\kappa_i) e^{iG_1 b x_0^2} \mathrm{sinc}\left(\frac{\Delta\beta L}{2}\right) e^{-i\frac{\Delta\beta L}{2}} \hat{a}_s^\dagger \hat{a}_i^\dagger |0,0\rangle. \tag{9}$$

Here we consider all the channels are pumped. According to Glauber's theory, the spatial coincidence counts outside the WA are calculated following

$$R_{c.c.}(x,z) \propto \langle\Psi|E_1^{(-)}E_2^{(-)}E_2^{(+)}E_1^{(+)}|\Psi\rangle, \tag{10}$$

where $E_2^{(+)}, E_1^{(+)}$ represents the field received by the single-photon detector 1 or 2 for the signal or idler photon after propagating a distance z from the back face of the WA. And these fields are written as

$$E_1^{(+)}(x_1,x_0) = \int\int d\omega_1 d\kappa_1 e^{-i\omega_1 t_1} \frac{e^{\frac{i\omega_1 z}{c}}}{z} \times \int dx_0 e^{i\kappa_1 x_0} e^{i\frac{\omega_1}{2cz}(x_1-x_0)^2} \hat{a}_1, \tag{11}$$

$$E_2^{(+)}(x_2,x_0') = \int\int d\omega_2 d\kappa_2 e^{-i\omega_2 t_1} \frac{e^{\frac{i\omega_2 z}{c}}}{z} \times \int dx_0' e^{i\kappa_2 x_0'} e^{i\frac{\omega_2}{2cz}(x_2-x_0')^2} \hat{a}_2. \tag{12}$$

These two fields are annihilated at space-time points (x_1,t_1) and (x_2,t_2), respectively. By substituting Eqs. (9), (11), and (12) into Eq. (10), we get

$$R_{c.c.} = \left|\int dx_0 A_p(x_0) e^{i(\frac{\omega_p}{2cz} - G_1 b)x_0^2} e^{-i\frac{\omega_p}{cz} x x_0}\right|^2. \tag{13}$$

When $z = \frac{\omega_p}{2cbG_1}$, we get

$$R_{c.c.} = \left|\int dx_0 A_p(x_0) e^{-i\frac{\omega_p}{cz} x x_0}\right|^2. \tag{14}$$

Specifically, we have

$$R_{c.c.} \sim \begin{cases} |\mathrm{sinc}(\frac{bwG_1}{\pi}x)\mathrm{comb}(\frac{bdG_1}{\pi}x)|^2 \text{ for infinite } N, \\ |[\mathrm{sinc}(\frac{bwG_1}{\pi}x)\mathrm{comb}(\frac{bdG_1}{\pi}x)] * \mathrm{sinc}(\frac{NbdG_1}{\pi}x)|^2 \text{ for finite } N. \end{cases} \tag{15}$$

This indicates that when the two detectors locate in the plane $z = f_{\mathrm{eff}} = \frac{\omega_p}{2cbG_1}$, defined as the self-focusing plane, the photon pair will focus into a series spot, meaning a high two-photon probability in these spots. The number of focused spots depends on the ratio of d and w mathematically. Usually, d cannot be too large since an efficient coupling between adjacent waveguides is required here; therefore, only several two-photon focusing spots can be observed. This two-photon self-focusing effect after the parabolic WA can be utilized to connect the WA and fibers by properly designing the effective focusing length.

VI. DISCUSSION

When considering the practical engineering of quantum states from the nonlinear WA, the loss should be taken into account since the loss may affect the degree of entanglement. Actually the loss in the nonlinear WA may lie at three aspects. First, the coupling loss of the pump when it is guided into the chip. For a linear WA, the entangled photons are seeded externally and experience such coupling loss inevitably. This will decrease the coincidence counting rate and even the fidelity of a quantum operation, while for the nonlinear WA, the entangled photon pairs are generated inside the chip and the loss only decreases the pump energy and therefore the photon pair rate, but will not affect the coincidence counting rate, which shows the advantage of nonlinear WA over the linear one. Secondly, the propagation loss in the waveguide exists. This is mainly decided by the fabrication technology. Unless the propagation loss reaches a low value [25,26], the two-photon amplitude in each waveguide can be considered identical, which will meet the requirement in the theoretical model. The third type of loss comes from the nonlinearity engineering. The domain engineering will definitely introduce some inhomogeneity or defects, thus causing some loss. But according to some experiments [27,28], the engineering loss in each waveguide can be considered as the same since it has been testified for transforming the spatial entanglement, and thus will not bring obvious impacts on the two-photon state.

VII. CONCLUSION

In this work, the $\chi^{(2)}$-modulated LN or LT waveguide array is proposed as a specific platform for engineering the two-photon state in a high-dimensional Hilbert space. By varying the pump condition and the WA length, the momentum correlation between the signal and idler photon can be manipulated, resulting in bunching, antibunching, and the evolution between these two states. The Schmidt number is calculated as a characterization of the degree of entanglement. We find a single structure parameter $(L/L_z)/N$ which uniquely determines the degree of entanglement especially for odd N and large even N. The degree of spatial entanglement shows the relevance with the linear profile of $\chi^{(2)}$ modulation, in which a high degree of the position-bunching state is suggested. Furthermore, the two-photon self-focusing effect is disclosed when the $\chi^{(2)}$ modulation in the WA contains a parabolic profile. These results indicate an on-chip engineering of the two-photon state in the WA dispensing with additional dealing of the pump beam, which will play the key role in the integrated quantum optics. Besides, such WA array can further be designed to engineer photons' other degrees of freedom, permitting the generation, transmission, and manipulation of photons to be accommodated on a single chip [29,30].

ACKNOWLEDGMENTS

This work was supported by the State Key Program for Basic Research in China (Grants No. 2012CB921802 and No. 2011CBA00205), the National Natural Science Foundations of China (Contracts No. 91321312, No. 91121001, No. 11321063, and No. 11174121), and the Project Funded by the Priority Academic Program development of Jiangsu Higher Education Institutions (PAPD). P.X. also acknowledges the Program for New Century Excellent Talents in University (NCET).

[1] D. N. Christodoulides, F. Lederer, and Y. Silberberg, Nature (London) **424**, 817 (2003).
[2] F. Lederer, G. I. Stegeman, D. N. Christodoulides, G. Assanto, M. Segev, and Y. Silberberg, Phys. Rep. **463**, 1 (2008).
[3] U. Peschel, T. Persch, and F. Lederer, Opt. Lett. **23**, 1701 (1998).
[4] T. Pertsch, P. Dannberg, W. Elflein, A. Brauer, and F. Lederer, Phys. Rev. Lett. **83**, 4752 (1999).
[5] R. Morandotti, U. Peschel, J. S. Aitchison, H. S. Eisenberg, and Y. Silberberg, Phys. Rev. Lett. **83**, 4756 (1999).
[6] D. Neshev, E. Ostrovskaya, Y. Kivshar, and W. Krolikowski, Opt. Lett. **28**, 710 (2003).
[7] H. Martin, E. D. Eugenieva, Z. Chen, and D. N. Christodoulides, Phys. Rev. Lett. **92**, 123902 (2004).
[8] R. Iwanow, D. A. May-Arrioja, D. N. Christodoulides, G. I. Stegeman, Y. Min, and W. Sohler, Phys. Rev. Lett. **95**, 053902 (2005).
[9] S. Longhi, M. Marangoni, M. Lobino, R. Ramponi, P. Laporta, E. Cianci, and V. Foglietti, Phys. Rev. Lett. **96**, 243901 (2006).
[10] I. L. Garanovich, A. A. Sukhorukov, and Y. S. Kivshar, Phys. Rev. E **74**, 066609 (2006).
[11] R. Iyer, J. S. Aitchison, J. Wan, M. M. Dignam, and C. M. de Sterke, Opt. Express **15**, 3212 (2007).
[12] A. Szameit, I. L. Garanovich, M. Heinrich, A. A. Sukhorukov, F. Dreisow, T. Pertsch, S. Nolte, A. A. Tnnermann, and Y. S. Kivshar, Nature Phys. **5**, 271 (2009).
[13] K. G. Makris, D. N. Christodoulides, O. Peleg, M. Segev, and D. Kip, Opt. Express **16**, 10309 (2008).
[14] K. Shandarova, C. E. Ruter, D. Kip, K. G. Makris, D. N. Christodoulides, O. Peleg, and M. Segev, Phys. Rev. Lett. **102**, 123905 (2009).
[15] H. B. Perets, Y. Lahini, F. Pozzi, M. Sorel, R. Morandotti, and Y. Silberberg, Phys. Rev. Lett. **100**, 170506 (2008).
[16] Y. Bromberg, Y. Lahini, R. Morandotti, and Y. Silberberg, Phys. Rev. Lett. **102**, 253904 (2009).
[17] A. Peruzzo, M. Lobino, J. C. F. Matthews, N. Matsuda, A. Politi, K. Poulios, X. Q. Zhou, Y. Lahini, N. Ismail, K. Worhoff, Y. Bromberg, Y. Silberberg, M. G. Thompson, and J. L. OBrien, Science **329**, 1500 (2010).
[18] A. S. Solntsev, A. A. Sukhorukov, D. N. Neshev, and Y. S. Kivshar, Phys. Rev. Lett. **108**, 023601 (2012).
[19] A. S. Solntsev, A. A. Sukhorukov, D. N. Neshev, and Y. S. Kivshar, Opt. Express **20**, 27441 (2012).
[20] R. Kruse, F. Katzschmann, A. Christ, A. Schreiber, S. Wilhelm, K. Laiho, A. Gabris, C. S. Hamilton, I. Jex, and C. Silberhorn, New J. Phys. **15**, 083046 (2013).
[21] C. K. Law and J. H. Eberly, Phys. Rev. Lett. **92**, 127903 (2004).
[22] M. P. van Exter, A. Aiello, S. S. R. Oemrawsingh, G. Nienhuis, and J. P. Woerdman, Phys. Rev. A **74**, 012309 (2006).
[23] A. Gatti, T. Corti, E. Brambilla, and D. B. Horoshko, Phys. Rev. A **86**, 053803 (2012).
[24] W. P. Grice, R. S. Bennink, D. S. Goodman, and A. T. Ryan, Phys. Rev. A **83**, 023810 (2011).
[25] K. R. Parameswaran, M. Fujimura, M. H. Chou, and M. M. Fejer, IEEE Photon. Technol. Lett. **12**, 654 (2000).
[26] C. Langrock, S. Kumar, J. E. McGeehan, A. E. Willner, and M. M. Feijer, J. Lightw. Technol. **24**, 2579 (2006).
[27] X. Q. Yu, P. Xu, Z. D. Xie, J. F. Wang, H. Y. Leng, J. S. Zhao, S. N. Zhu, and N. B. Ming, Phys. Rev. Lett. **101**, 233601 (2008).
[28] H. Y. Leng, X. Q. Yu, Y. X. Gong, P. Xu, Z. D. Xie, H. Jin, C. Zhang, and S. N. Zhu, Nat. Commun. **2**, 429 (2011).
[29] M. F. Saleh, G. Di Giuseppe, B. E. Saleh, and M. C. Teich, Opt. Express **18**, 20475 (2010).
[30] M. F. Saleh, B. E. Saleh, and M. C. Teich, Phys. Rev. A **79**, 053842 (2009).